

Electronic Supplementary Information

Superhydrophobic Surfaces with Fluorinated Cellulose Nanofiber Assemblies for Oil–Water Separation

M. Mahbubul Bashar, Huie Zhu, Shunsuke Yamamoto and Masaya Mitsuishi
Institute of Multidisciplinary Research for Advanced Materials
Tohoku University, 2-1-1 Katahira, Aoba-ku, Sendai 980-8577, Japan

1. Relative intensity of CF₂ group in modified CNF

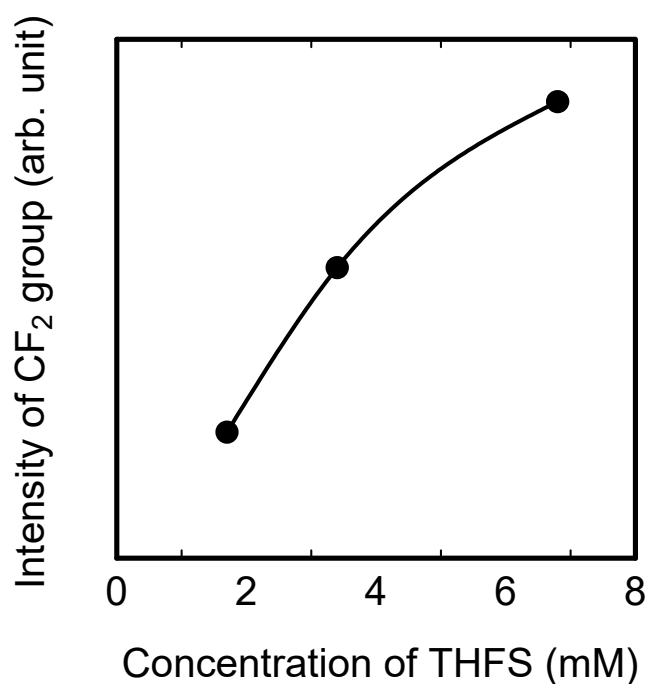


Figure S1. Relative peak intensity of CF₂ chain in modified CNF as a function of THFS concentration.

Figure S1 presents the relative intensity of CF₂ chain in modified CNF. The intensity was calculated from the FT-IR absorption peak intensity of CF₂ group at 1235–1205 cm⁻¹ and cellulosic main peak at 1160–1034 cm⁻¹ regions. The intensity increased almost linearly with increased concentration of THFS, with three concentrations of *ca.* 1.7, 3.4, and 6.8 mM.

2. Characteristic peak of hydroxyl group in CNF

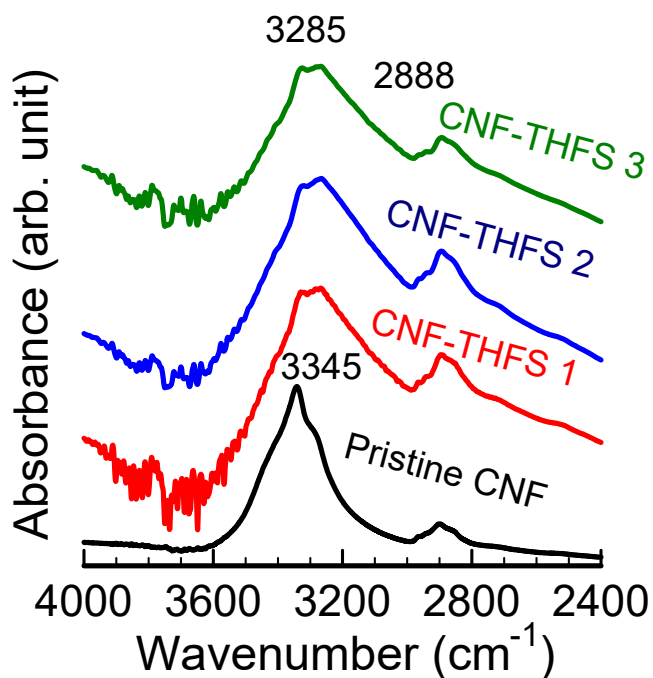


Figure S2. FT-IR spectra of pristine and modified CNF indicating a shifting peak of –OH group to the lower band as a consequence of incorporation of fluorine chain into the CNF backbone. Numbers 1, 2, and 3 respectively denote concentrations of THFS 1.7, 3.4, and 6.8 mM.

3. High-resolution Si 2p spectra of modified CNF assemblies

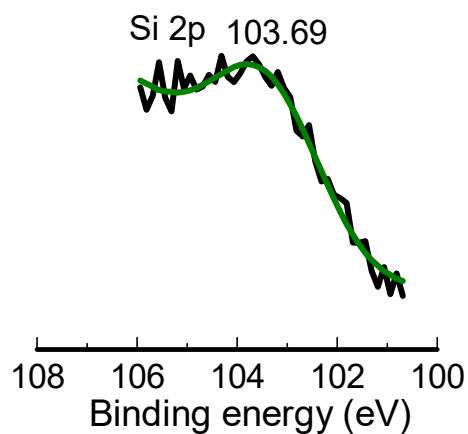


Figure S3. High-resolution Si 2p spectra of the modified CNF assembly surface.

4. Surface wettability of the modified CNF assembly surface

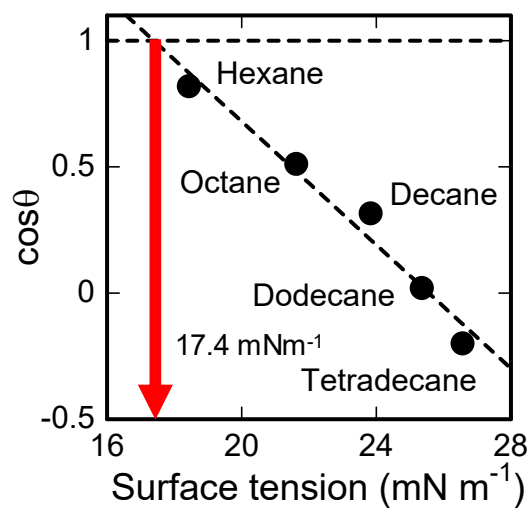


Figure S4. Critical surface energy of the modified CNF assembly surface.

To measure the surface tension of the modified CNF surface, the contact angles of hexane, octane, decane, dodecane, and tetradecane were measured. An almost linear relation was observed between the contact angle and the surface tension of alkanes. By extrapolation of the linear plot to $\cos\theta_c$ equal to 1, the critical surface tension (γ_c) was calculated according to the method described by Zisman.⁵¹ Figure S4 presents the critical surface tension of the modified CNF surface 17.4 mNm^{-1} .

5. Adhesion force of the modified CNF assembly surface

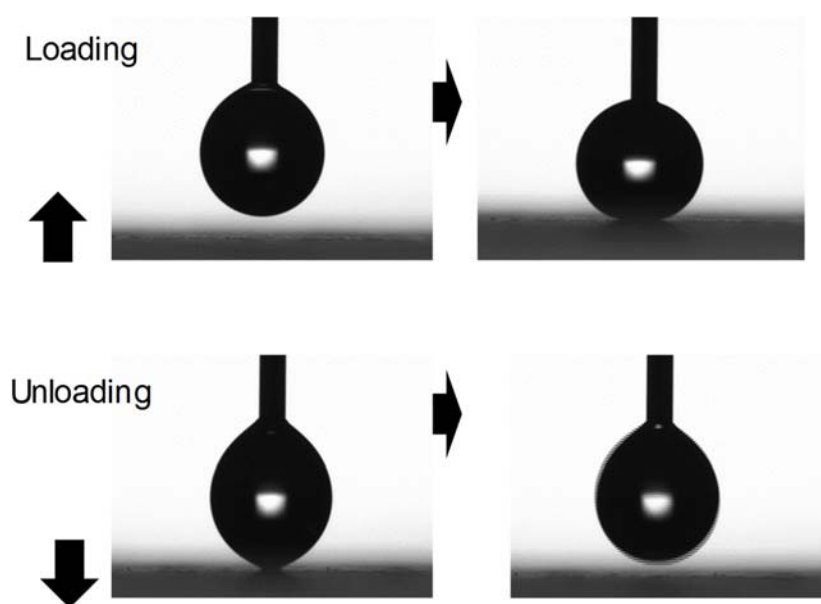


Figure S5. Photographs of water droplets on the modified CNF assembly surface for (top) loading and (bottom) unloading.

6. Snapshots of water droplet bounced on the modified CNF assembly surface

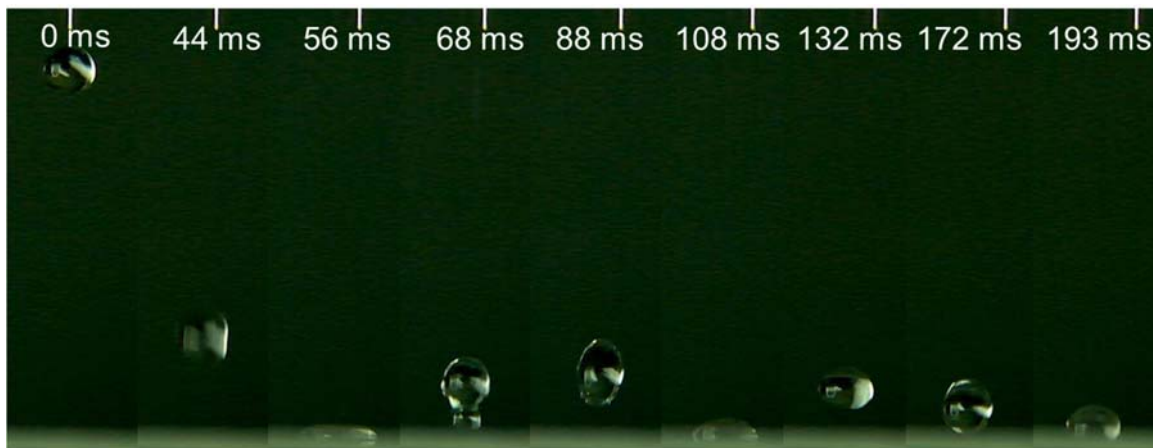


Figure S6. Photographs of water droplet (20 L) bounced on the modified CNF assembly surface.

Snapshots were taken at a 250 fps frame rate by using a motion analyzing microscope (VW-6000; Keyence Co.) equipped with a lens (VW-Z2).

7. Micro–nanostructure of drop-coated modified CNF

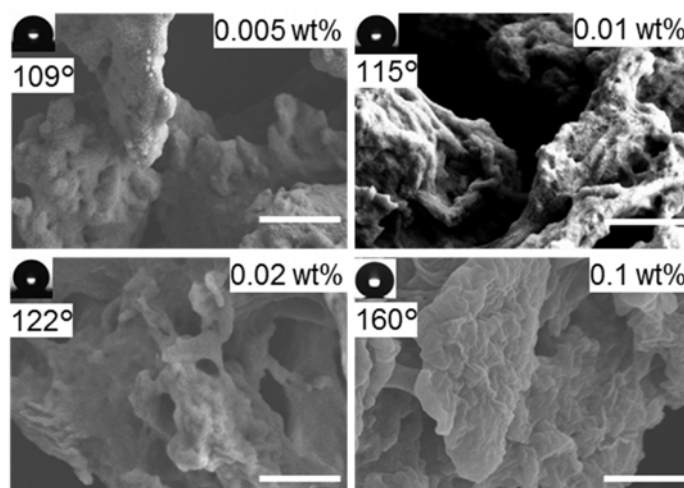


Figure S7. Nanostair geometrical architecture appeared as a function of the concentration of the modified CNF suspension. The scale bar is 1 μm for all images. Inset figures show WCA on modified CNF-coated Si substrates.

8. Fractional area covered by water droplet on modified CNF assembly surfaces

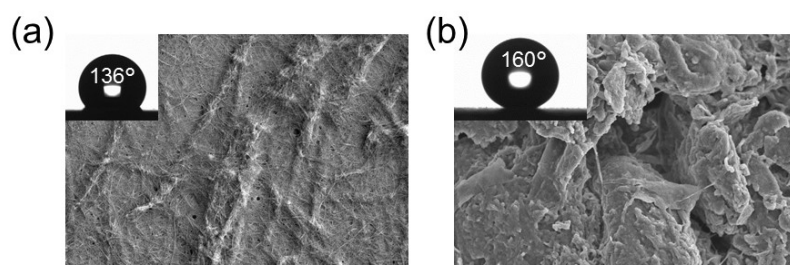


Figure S8. FE-SEM images of (a) drop-coated pristine CNF assembly dipped into 6.8 mM THFS for 8 h and (b) drop-coated assembly surface of modified CNF. Inset figures portray the WCA. The scale bar is 10 μm .

The water contact angle of superhydrophobic CNF surfaces can be interpreted according to

Cassie–Baxter model as

$$\cos\theta_r = f(\cos\theta + 1) - 1 \quad (1)$$

where θ_r represents the apparent contact angle on a superhydrophobic porous surface, θ denotes the equilibrium contact angle on the flat surface, and f corresponds to the area fraction of the liquid–air interface in the case of the modified CNF surface. Furthermore, θ_r was determined as 160°. The contact angle on the flat surface was calculated as 110° using a THFS self-assembled monolayer. For comparison, another surface was prepared as follows. First the 0.1 wt% water suspension of pristine CNF was drop-coated onto Si substrate and dried at 60°C for 24 h; then it was immersed in 6.8 mM AK-225 solution of THFS and kept

for 8 h. After the sample was washed in AK-225 to remove unreacted THFS, it was dried under vacuum (post-modified treatment). Using equation (1) above, $f = 0.908$ was obtained for the modified CNF assembly surface; $f = 0.573$ for the post-modified CNF assembly surface. Results indicate that about 90.8% of the area is occupied by the liquid–air interface and that the pre-surface modification is more effective for superhydrophobic surface preparation.

9. Film thickness measurement of superhydrophobic CNF assemblies

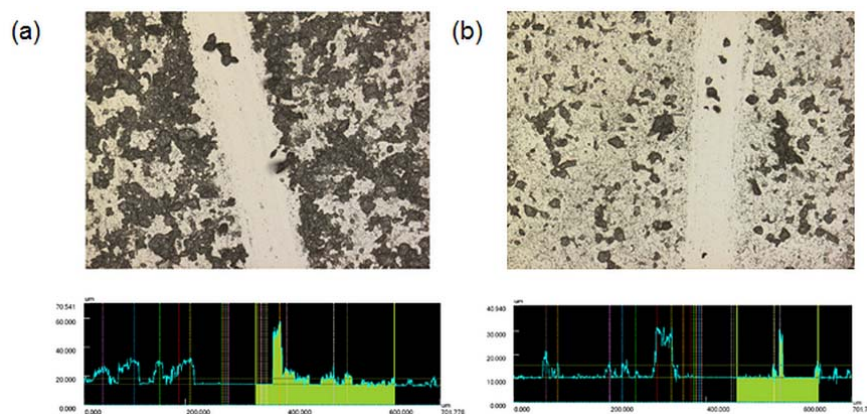


Figure S9. Top and cross-sectional views of modified CNF assemblies coated with (a) 1 mL and (b) 0.5 mL 0.1 wt% modified CNF suspension from AK-225 with the corresponding height profile by optical laser microscope.

Modified CNF 0.1 wt% suspension in AK-225 was drop-coated onto quartz substrates by 0.5 mL and 1 mL solution. The coated substrates were dried under vacuum for 8 h. The film thickness was measured using a laser scanning microscope (VK-9700; Keyence Co.,

Japan). Figure S9 shows top and cross-sectional views of the surfaces. The thickness was found by measurement at 10 positions. Average values were 14.95 and 9.31 μm , respectively, for 1 mL and 0.5 mL drop-coated surfaces.

10. Thermogravimetric (TGA) analysis

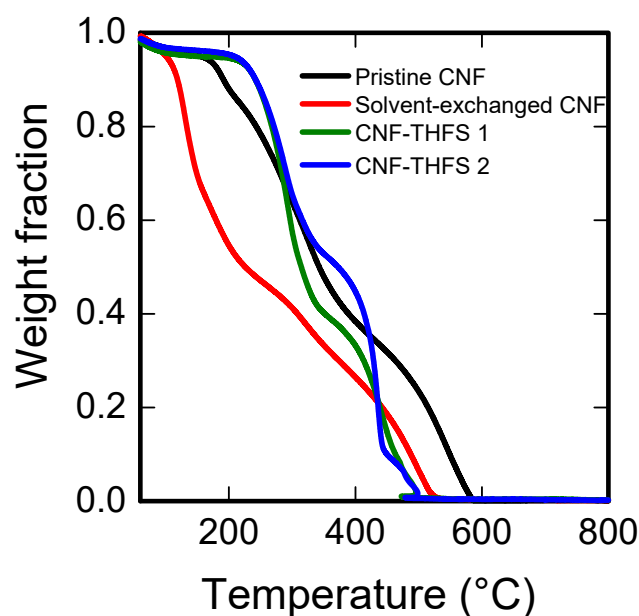


Figure S10. TGA curves of pristine, solvent exchanged, and modified CNF for different conditions. Numerical values 1 and 2 respectively denote molar concentrations of THFS 3.4 and 6.8 mM.

Figure S10 presents TGA curves of pristine, solvent exchanged CNF, and modified CNFs. The solvent exchanged CNF showed less stability during heating. Generally, CNF is crystalline polymer, with good thermal stability because CNF chains are mutually connected through intramolecular and intermolecular hydrogen bonding, thereby making it a rigid polymer.⁵²

However, when water was removed by solvent exchange, the thermal behavior changed drastically. The modified CNF showed better thermal stability than pristine CNF at 180–220 °C. The 5% weight loss temperature (Td_5) of pristine CNF was 180 °C, whereas the values were found to be 230–235 °C for modified CNFs. The reason for improved thermal stability of modified CNF might be incorporation of fluorinated ligands into cellulose nanofiber surfaces, which results in crosslinking.

11. Chemical stability of superhydrophobic CNF assembly surfaces

Figure 7(b) displays the chemical stability of the modified CNF surfaces with artificial seawater, and with highly acidic and alkaline water solutions. Artificial seawater was prepared by dissolving 3.5% NaCl in deionized water. Substrates were immersed in the solution for 5 min. Then, they were rinsed in water and were dried in vacuum. The study confirmed that the modified CNF assembly surface is stable under severe environmental conditions.

12. Wettability of organic hydrocarbons

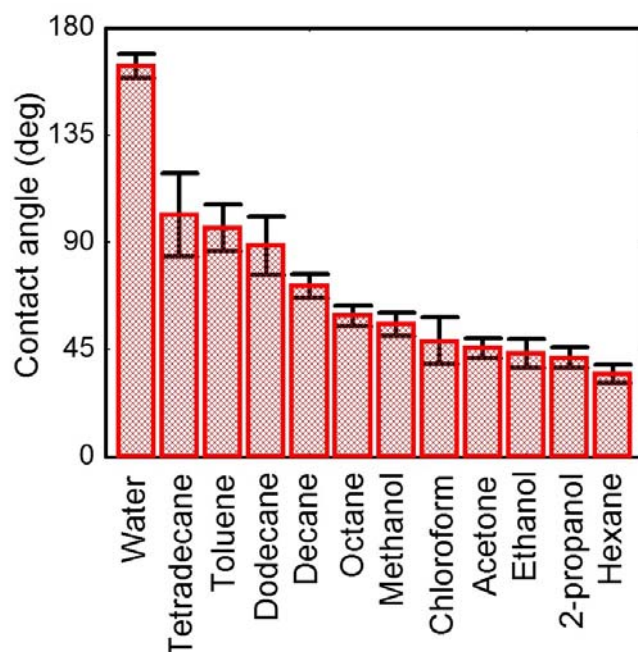


Figure S11. Contact angles of different hydrocarbons and organic solvents on modified CNF assembly surfaces.

13. FE-SEM images of uncoated and coated steel mesh

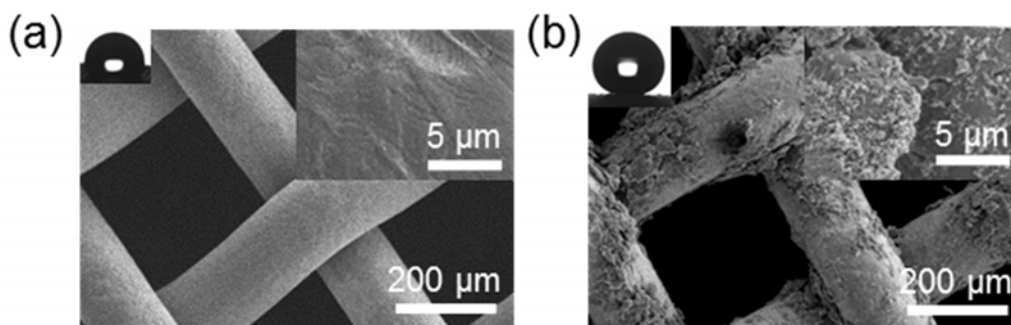


Figure S12. FE-SEM images of (a) bare steel mesh with 150 μm mesh pore size. The right inset shows a high magnification image of the smooth surface with WCA of 110° (left inset) (b) modified CNF coated steel mesh giving hierarchical micro-nano roughness (right inset) with WCA of 162° (left inset).

14. Separation efficiency for different organic solvents

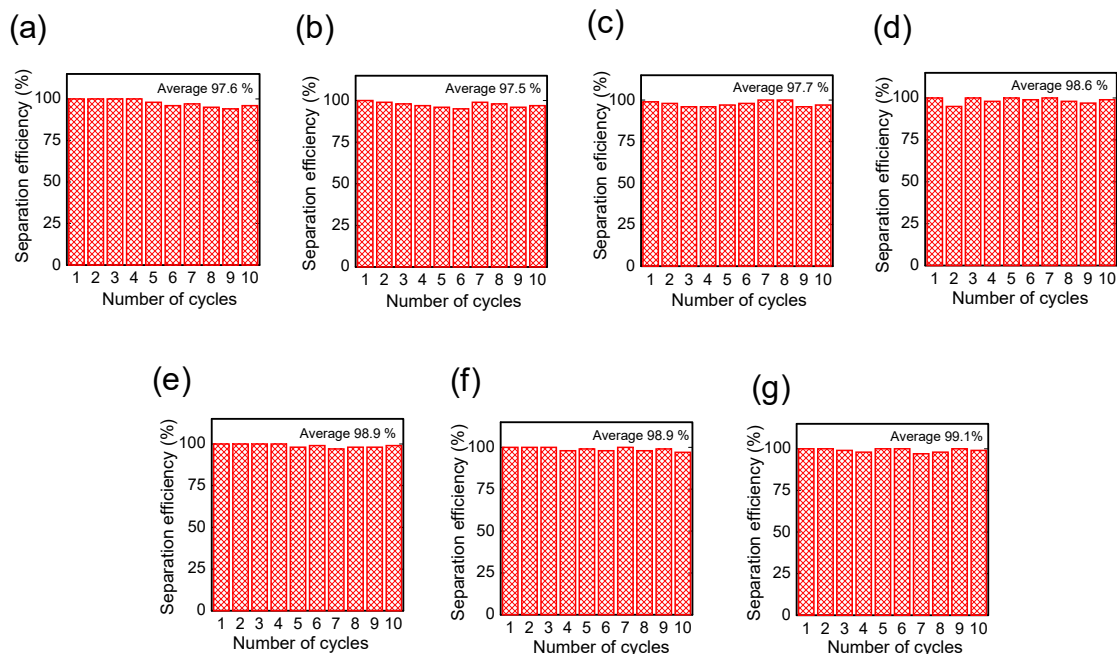


Figure S13. Separation efficiency of different organic solvents as a function of the number of cycles; (a) toluene, (b) tetradecane, (c) dodecane, (d) decane, (e) kerosene, (f) octane and (g) hexane.

15. Component of surface free energy of modified CNF assembly surfaces.

The surface free energies (SFEs) of modified CNF, pristine CNF, and self-assembled monolayer (SAM) of THFS were evaluated using Owens and Wendt method with the following equation.

$$\frac{1}{2}\gamma_l(1 + \cos \theta) = \sqrt{\gamma_l^p \gamma_s^p} + \sqrt{\gamma_l^d \gamma_s^d} \quad (2)$$

Therein, γ_l and γ_s respectively represent the surface tension of the liquid and solid; θ denotes the contact angle. Superscripts p and d respectively denote polar and non-polar

components of surface tension. The contact angles of water and decane were measured on pristine CNF, modified CNF, and SAM of THFS as presented in Table S1. Using parameters $\gamma_{water}^p=51.0$ mN/m, $\gamma_{water}^d=21.8$ mN/m, $\gamma_{decane}^p=0$ mN/m, and $\gamma_{water}^d=23.8$ mNm⁻¹, the SFE components were calculated as presented in Table S2.

Table S1. Contact angles of different surfaces for water and decane

Surfaces	Contact angle (deg)	
	Water	Decane
Pristine CNF	25.5	7
SAM of THFS	110.27	62.84
Modified CNF	164	71.55

Table S2. Components of surface free energy of different surfaces

Surfaces	Component of surface free energy (mNm ⁻¹)	
	Dispersion	Polar
Pristine CNF	23.62	42.52
SAM of THFS	12.62	1.01
Modified CNF	10.31	3.62

References

(S1) H. W. Fox and W. A. Zisman, *J. Colloid. Sci.* 1950, **5**, 514.

(S2) R. J. Moon, A. Martini, J. Nairn, J. Simonsen and J. Youngblood, *Chem. Soc. Rev.* 2011, **40**, 3941.